International Journal of Machine Tools & Manufacture 85(2014) pp. 100–121

http://dx.doi.org/10.1016/j.ijmachtools.2014.05.005

ELSEVIER journal homepage: www.elsevier.com/locate/ijmactool

A Review of Process Advancement of Novel Metal Spinning

Qinxiang Xia[a*], Gangfeng Xiao[a], Hui Long[b], Xiuquan Cheng[c], Xiangfei Sheng[a]

[a]School of Mechanical and Automotive Engineering, South ChinaUniversity of Technology, China

[b]Department of Mechanical Engineering, The University of Sheffield, UK

[c]Department of Aircraft Maintenance Engineering, Guangzhou Civil Aviation College, China

[*]Correspondence, E-mail address: meqxxia@scut.edu.cn (Q. Xia).

Abstract

Metal spinning technology has seen a rapid development in recent years. Novel spinning processes, such as non-axisymmetric spinning, non-circular cross-section spinning and tooth-shaped spinning, are being developed. This has challenged the limitation of traditional spinning technology being used for manufacturing axisymmetric, circular cross-section, and uniform wall-thickness parts. In this paper, the classification of the traditional spinning processes is proposed based on the material deformation characteristics, the relative position between roller and blank, mandrel spinning and mandrel-free spinning, and temperature of the blank during spinning. The advancement of recently developed novel spinning processes and corresponding tool design and equipment development are reviewed. The classification of the novel spinning processes is proposed based on the relative position between the rotating axes, the geometry of cross-section and the variation of wall-thickness of spun parts. The material deformation mechanism, processing failures and spun part defects of the aforementioned three groups of novel spinning processes are discussed by analyzing four representative spinning processes of industrial applications. Furthermore other novel spinning processes and their classification as reported in the literature are summarized.

Keywords: Spinning**,** Non-axisymmetric spinning**,** Non-circular cross-section spinning**,** Tooth-shaped spinning.

Nomenclature

P	resultant spinning force of the roller
P_z, P_r, P_t	spinning force components of the roller along the axial, radial and tangential direction
$\sigma_{c,z}$, $\sigma_{c,r}$	average axial and radial contact stresses between the roller and the workpiece
A_z, A_r	projective axial and radial contact areas between the roller and the workpiece
δ	offset value
φ	oblique angle
γ	rotational angle of the roller
r_ρ	roundness radius of the roller
f	feed rate of the roller
D_r	diameter of the roller
D_0	original diameter of the tubular blank
D	diameter of the tubular workpiece after each roller path
Δ	nominal reduction of the blank radius per path, $\Delta = (D_0 - D)/2$
S	distance from the revolution plane of the roller to the datum plane
β'	installation angle of the roller
t_0	initial thickness of the blank
D_0'	diameter of the circumscribed circle of the blank
t_0/D_0'	thickness-diameter ratio of the blank
P_{zmax}, P_{rmax}, P_{tmax}	maximum roller force components along the axial, radial and tangential direction
h	height of the workpiece during spinning
n	rotational speed of the mandrel
C	clearance between the mandrel and the roller
ΔC	relative clearance between the mandrel and the roller, $\Delta C = 100\%(C-t_0)/t_0$
f_z	feed rate of the roller along the axial direction
t_f	wall thickness of the workpiece

δ_t	maxmum thinning ratio of the wall thickness
α	semi-cone angle of the workpiece
α_0	semi-cone angle of the mandrel
$\Delta\alpha$	springback angle of the workpiece, $\Delta\alpha=\alpha-\alpha_0$

1. Introduction

Metal spinning is one of the near-net shape forming processes widely used for manufacturing axisymmetric, thin walled-thickness and hollow circular cross-section parts. The process involves the feeding motion of one or more rollers against a metal blank or tube rotating together with the main spindle of a machine to obtain desired axisymmetrical and hollow geometries by inducing continuous and localized plastic deformation on the blank or tube [1]. Due to the nature of localized material deformation, this process has inherent advantages, such as low forming loads, simple tooling, good dimensional accuracy, high material utilization, low production costs and improved mechanical properties, be apt to obtain lightweight parts with flexibility in manufacturing. Metal spinning in modern times has been widely used in various industries requiring high precision material processing, such as aviation, aerospace, automotive, defence, medical, energy and electronics industry. Spinning process is capable of forming components of diameter ranging from 3 mm to 10 m, and thicknesses from 0.4 to 25 mm [2, 3].

In recent years, novel spinning processes are being developed which challenges the limitation of traditional spinning technology being used for manufacturing axisymmetric, circular cross-section, and uniform wall-thickness parts [2, 4]. Xia [5] developed a 3D non-axisymmetric spinning process, in which the workpiece was free from the rotational motion during processing and the roller set was installed on the main spindle and rotated together with the main spindle of the machine. Using the developed process a thin-walled hollow part with a partial axis paralleling or being a certain inclined angle to the original axis of the workpicec can be produced without the need of using subsequent welding processes. Awiszus et al. [6, 7] developed a non-circular spinning process, thin-walled hollow parts with tripod shaped cross-section were manufactured, by a standard spinning lathe with a pair of diametrically opposite, spring-controlled rollers. Schmoeckel and Hauk [8] proposed a new flow-splitting spinning method, where the tool configuration design consisted of one splitting roll and two supporting rolls, and the distance between the splitting roll and each supporting roll was adjusted to a specified value, therefore overcame the limitation of attainable radial splitting depths successfully. Xia et al. [9] developed a stagger inner gear spinning method, where three rollers were 120º equally positioned along the circumference of

the workpiece and there was a certain distance between rollers along both the axial and radial directions of the workpiece. The method has been successfully used to form various cup-shaped thin-walled inner gears [9]. The development of these novel spinning processes has broadened the scope of the traditional spinning technology being used to manufacture axisymmetric, circular cross-section, and uniform wall-thickness parts for various industrial applications. However, these newly developed spinning processes do not belong to any existing spinning processes if using the traditional classification method, thus the classification of the recently developed novel spinning processes is necessary. In this paper, the advancement of novel spinning processes is reviewed and a classification of the non-axisymmetric spinning, non-circular cross-section spinning, and tooth-shaped spinning is proposed. Examples of industrial applications of the novel spinning processes are analysed to provide an insight into the material deformation characteristics during forming.

2. Classification of traditional spinning processes

The classification of the traditional spinning processes has been developed mainly according to the deformation characteristics of the blank material, the relative position between the roller and the blank, spinning with or without mandrel, and the temperature of the blank. The classification is usually based on the following four methods:

2.1. Conventional spinning and power spinning-Method 1

According to the deformation characteristics of the blank material, spinning can be divided into conventional spinning and power spinning or compression forming and flow forming [1]. In conventional spinning or compression forming, the wall-thickness of the blank remains nearly constant throughout the process, thus the final wall-thickness of the spun part is equal to the thickness of the blank [2]. In contrast, the wall-thickness of the blank is reduced in power spinning or flow forming. Power spinning or flow forming is further divided into shear spinning for conical parts and flow spinning for tubular parts. The shear spinning is characterized by the fact that the radial position of an element in the blank remains the same during material deformation. This requires that the initial thickness of the blank t_0 and the final thickness of the conical shell t_f are correlated by the sine law, $t_f = t_0 \sin\alpha$, where α is the semi-cone angle of the workpiece [10]. In flow spinning, the final thickness is related to the increase in length of the spun part [11], and it is further classified as forward and backward spinning [12]. While some researchers propose to classifty spinning into conventional spinning and flow forming, in this paper, the authors prefer the classification of conventional spinning and power spinning as the flow forming is now commonly used to refer to the tubular part spinning. **Fig. 1** outlines the classification of the traditional spinning

processes based on the deformation characteristics of the blank material.

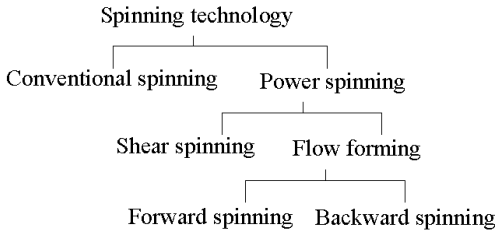

Fig. 1. Classification of traditional spinning processes based on deformation characteristics of the blank material.

2.2. Inner spinning and outer spinning-Method 2

According to the relative position between the roller and the blank, spinning can be divided into inner spinning and outer spinning (or necking spinning and expanding spinning) [13]. In traditional spinning, the mandrel is generally mounted inside of the blank, the roller presses the blank from the outside, the process is termed as outer spinning. However, in some special cases, such as expanding spinning as shown in **Fig. 2**, the relative position of roller and blank is exchanged, the roller presses the blank from the inside, thus the process is termed as inner spinning [14].

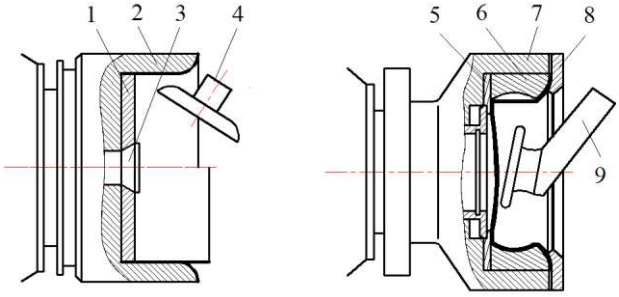

(a) spun part without bottom. (b) spun part with bottom.

1-Supporting plate 2-Outer spinning mandrel 3-Locking pin 4-Roller 5-Pushing plate

6-Combination spinning mandrel 7-Chuck 8-Jackcatch 9-Roller head

Fig. 2. Schematic of expanding spinning [13].

2.3. Mandrel spinning and mandrel-free spinning-Method 3

Depending on if a specific mandrel is used in the process, spinning can be divided into mandrel spinning and mandrel-free spinning. In traditional spinning, a specific mandrel is usually required for each product, the blank is clamped rigidly against the mandrel by means of a tailstock and the shape of the mandrel bears the final profile of the desired product [1]. However, when the reduction of the blank radius is too great or the opening end of a product requires to be necked or sealed by spinning, such as necking or sealing of a gas container as shown in **Fig**

3a [15], neck forming should be processed under the mandrel-free condition. Forthermore, in some special cases, such as spinning a blank with large dimension as shown in **Fig 3b** [16], an inner supporting roller is generally used to replace the mandrel in order to reduce the weight of the mandrel.

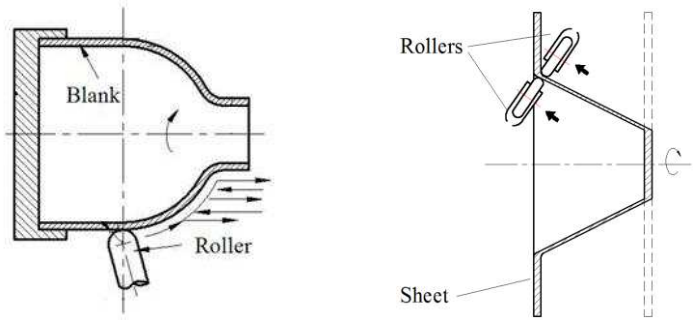

(a) neck-spinning. (b) spinning with a supporting roller.

Fig. 3. Schematic of mandrel-free spinning [15, 16].

2.4. Cold spinning and hot spinning-Method 4

Depending on the temperature of the blank during spinning, spinning can be divided into cold spinning (spinning at room temperature) and hot spinning (spinning above the recrystallization temperature) [17]. Conventional spinning processes are typically performed at room temperature, but for parts with large thickness and made of high strength materials which have poor ductility for cold spinning, heating is generally applied to the blank in order to reduce the forming forces required during spinning. A hot spinning process is attractive in forming brittle and high strength materials [2,18].

Summarizing the above four classification methods, the classification of the traditional spinning processes is presented in **Fig. 4**.

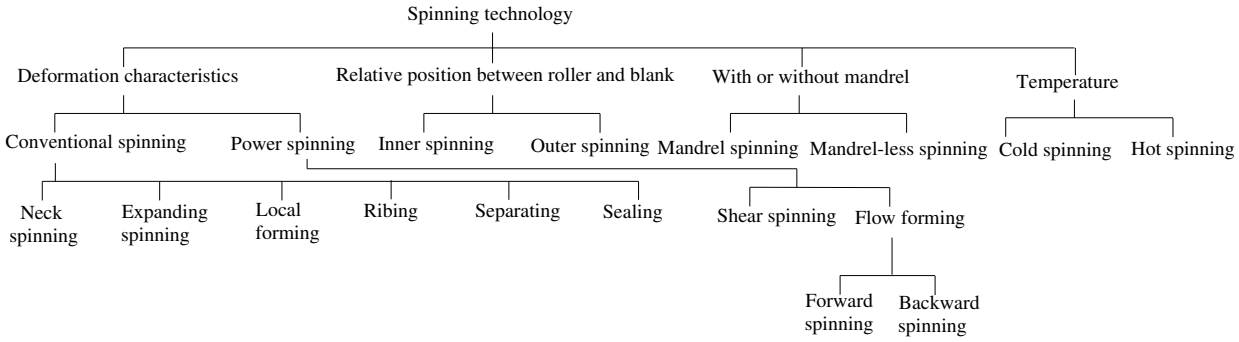

Fig. 4. Classification of traditional spinning processes.

3. Classification and analysis of material deformation mechanism of novel spinning processes

Different from the classication of traditional spinning processes as shown in Fig. 4, the classification of novel spinning processes is proposed based on (1) the relative position between the rotating axes, (2) the geometry of

cross-section, and (3) the variation of wall-thickness of spun part. According to the material deformation characteristics of the following three groups of novel spinning processes: non-axisymmetric spinning, non-circular cross-section spinning, tooth shaped spinning, the classification can be defined as:

3.1. Non-axisymmetric spinning-Method 1

Depending on the relative position between rotating axes of the spun part, novel spinning processes can be divided into axisymmetric spinning and non-axisymmetric spinning, the latter can be further subdivided into the offset spinning and the oblique spinning, as shown in **Fig. 5** [5]. In axisymmetric spinning, there is only one rotational axis of the spun part, the cross-section is circular, as shown in Fig. 5(a). In non-axisymmetric spinning, there are two or more rotational axes, one axis of the spun part may be parallel or tilted to other axes of the part, but the cross-section perpendicular to the rotational axis is still circular, as shown in Fig. 5(b).

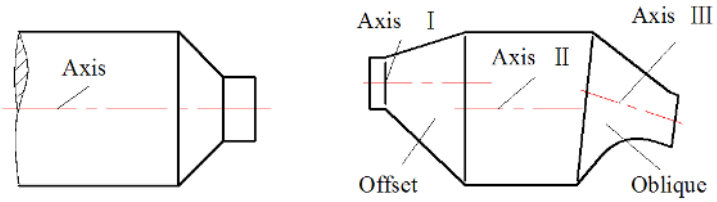

(a) axisymmetric. (b) non-axisymmetric.

Fig. 5. Axisymmetric and non-axisymmetric parts [5].

In the work reported by Xia et al. [19], during non-axisymmetric spinning, the tubular blank is fixed by the clamp, the manufacturing of non-axisymmetric parts can be realized using the spinning machine by the planetary motion of a wedge-shaped roller-set, the axial and radial feeding, and the rotation of the workpiece in the horizontal plane of the clamp, as shown in **Fig. 6**, while the offset or inclination of the blank is realized through the translation or rotational motion of the clamp. The three rollers, positioned 120º apart and uniformly distributed along the circumference of the blank, rotate with the main spindle of the machine and feed in the radial direction simultaneously. The alternating forward and backward path spinning method is proposed by Xia et al. [20,21], as shown in **Fig. 7**. The method not only shortens the production time, but also improves the dimensional accuracy of the spun part by generating the material deformation flow under improved control.

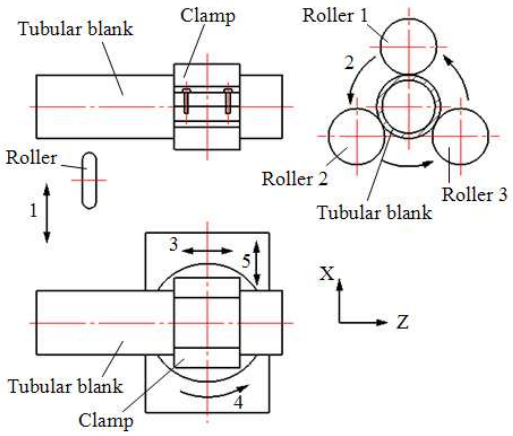

1-Radial feed of rollers 2-Revolution movement of rollers 3-Axial feed of clamp

4-Rotational motion of clamp 5-Radial translational movement of clamp

Fig. 6. Working principle of non-axisymmetric spinning [19].

For offset tube spinning, prior to spinning per path, firstly the tubular blank is offset at an required distance in the direction perpendicular to the axis of the blank, then during forming, the tubular blank is fed along the direction of rotating axis of the roller until the total offset of roller paths reaches the required amount δ_0, as shown in Fig. 7 (a) [22].

For oblique tube spinning, prior to spinning per path, firstly the tube blank is inclined at a specific angle in relation to the horizontal surface of workbench, then during forming, the tubular blank is allowed to move along the direction of the rotating axis of the roller until the total oblique angle reaches the required amount φ_0 after several roller paths, as shown in Fig. 7 (b) [23].

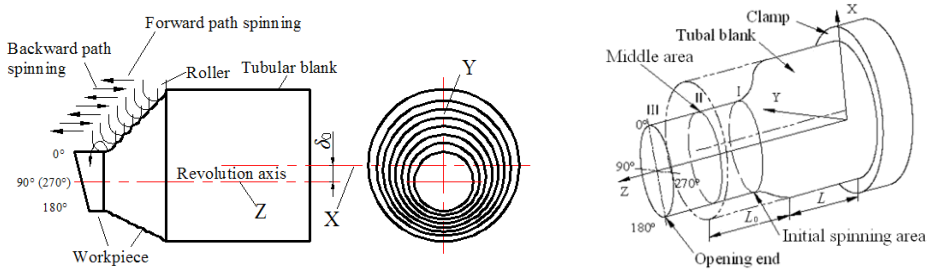

(a) offset tube.

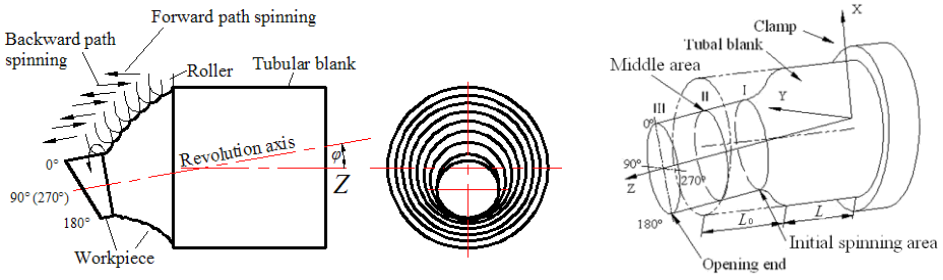

(b) oblique tube.

Fig. 7. Schematic of non-axisymmetric spinning process [20].

As reported by Xia et al. [20], the distributions of equivalent stresses and strains are non-uniformly distributed during offset and obilique tube spinning. The location of the maximum equivalent stress and strain are at the 0° area (as shown in Fig.7) where the offset or inclination is the greatest (as shown in Fig.7); while the minimum equivalent stress and strain are at the 180° area (as shown in Fig.7). For the oblique tubes, the distribution of strains varies gradually along the axial direction, which is different from that of the offset tube.

The theoretical calculation formulas of the spinning forces for the offset tubes [22] and oblique tubes [23] were obtained based on the Slab Method. Xia et al. reported that in order to selecte sufficient power suppliers for the lateral and longitudinal servo-actuators, and the main motor of the spinning machine to meet the spinning process requirement, the spinning force P was decomposed to the radial, axial and tangential force components, P_r, P_z and P_t, as shown in **Fig. 8** [24].

$$P = \sqrt{P_r^2 + P_t^2 + P_z^2} \tag{1}$$

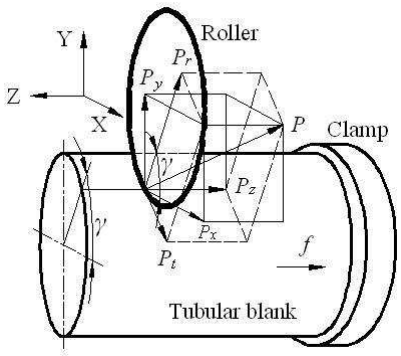

Fig. 8. Spinning force P and its components P_r, P_z and P_t [24].

Both the theoretical analysis and experimental measurements confirm that the tangential spinning force component is considerably small when comparing with the radial and axial spinning force components, the axial and radial spinning force components, P_r and P_z, can be calculated as follows [20, 22, 23]:

$$\begin{cases} P_r = \sigma_{c,r} A_r \\ P_z = \sigma_{c,z} A_z \end{cases} \tag{2}$$

where, $\sigma_{c,r}$ and $\sigma_{c,z}$ are the average radial and axial contact stresses between the roller and blank respectively; A_r and A_z are the projective radial and axial contact areas between the roller and blank, respectively, as shown in **Fig. 9**.

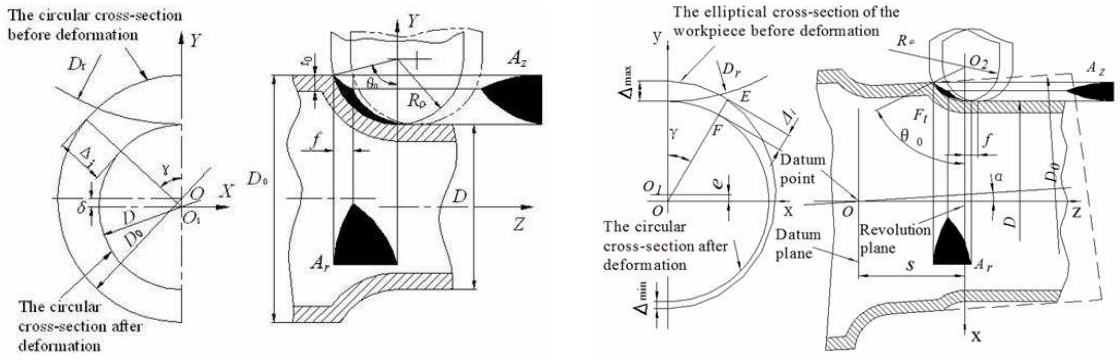

(a) offset tube spinning. (b) oblique tube spinning.

Fig. 9. Projective contact areas between roller and workpiece [22, 23].

Fig.10 shows the results of the variations of spinning force during non-axisymmetric tubes spinning obtained by the above theoretical calculations. It shows that during non-axisymmetric tubes spinning, spinning force components vary periodically along with one revolution of the roller rotating around the workpiece. **Fig.10 (a)** shows the effect of rotational angle of roller γ on P_r and P_z during offset spinning when roundness radius of the roller r_ρ=10 mm, feed rate of the roller f=1 mm/r, offset value δ=2.5 mm and nominal reduction of the blank Δ=5 mm. It shows that the maximum spinning force occurs at the position of γ=0º, and the minimum spinning force occurs at the position of γ=180º. **Fig.10 (b)** shows the effect of rotational angle of roller γ on spinning force during oblique spinning when feed rate of the roller f=1 mm/r, oblique angle φ=3º, nominal reduction of the blank Δ=3 mm and the distance from the revolution plane of the roller to the datum plane S=10 mm. It shows that during one revolution of the roller around the workpiece, the maximum and minimum spinning forces appear once respectively [25].

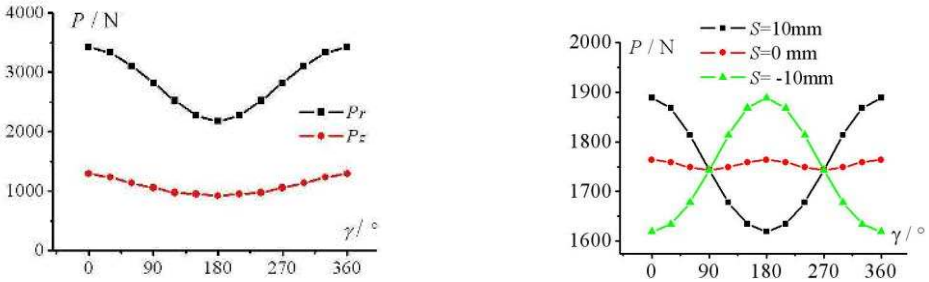

(a) offset spinning. (b) oblique spinning.

Fig.10. Effect of rotational angle of roller on spinning force [25].

3.2. Non-circular cross-section spinning-Method 2

According to the cross-section geometry of spun parts, the novel spinning processes can be divided into circular cross-section spinning and non-circular cross-section spinning. For a non-circular cross-section the radial distance

from the perimeter of the spun part to the geometric center of the cross-section is a variable, as shown in **Fig. 11**.

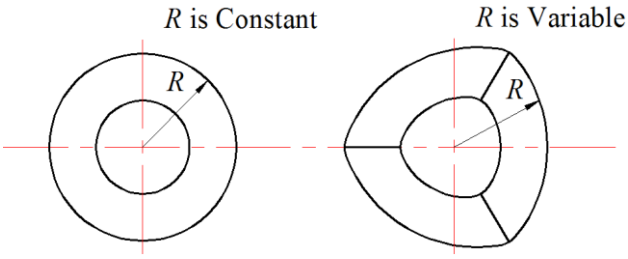

(a) circular cross-section. (b) non-circular cross-section.

Fig. 11. Circular cross-section and non-circular cross-section spun parts.

Research investigations based on many experiments have shown that the spinning processes can be successfully used to produce a variety of complex hollow parts with non-circular cross-sections [26]. Xia et al. developed a non-circular spinning method based on profiling driving method to produce various hollow parts with polygonal cross-sections, such as triangle arc-type cross-section [27], quadrilateral arc-type [28], and five straight-edge roundness-type [29]. Lai et al. [30] successfully produced hollow parts with three straight-edge roundness-type cross-sections, also based on the profiling driving method. Cheng et al. [31] reported that for the spinning of the circular cross-section parts, the roller should be fed along the radial direction of workpiece at a slow and constant speed. However, for the spinning of the non-circular cross-section parts, the radial feeding of roller varies because of the variation of distance from the edge of the part to the geometric center of cross-section of the mandrel [31].

In the work reported by Xia et al., as shown in **Fig. 12** [27], O_1 is the rotational center of the mandrel, O_2 is the center of the roller, ω_1 is the rotation speed of the mandrel, ω_2 is the rotation speed of the roller. When the roller is fed along the axial direction, it also has a high radial speed with reciprocated movement which results in dynamic behaviour of the roller interacting with the workpiece. It shows that during non-circular cross-section spinning, from the center of side-edge to the junction of two side-edges of arcs, the roller should be moved backward at a high speed as the increased distance from the edge of the part to the geometric center of cross-section of the mandrel; conversely, the roller should be moved forward at a high speed. To obtain a uniform wall thickness of spun part, the clearance between the mandrel and the roller should be set exactly the same as the blank thickness.

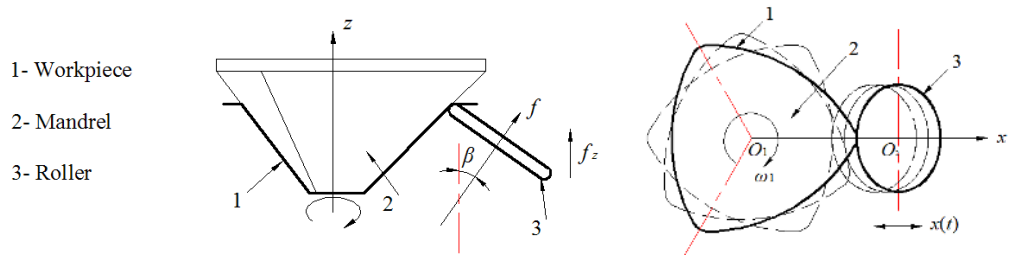

(a) axial section. (b) top view.

Fig. 12. Spinning of hollow-part with triangle arc-type cross section [27].

Fig.13 shows the hollow-part with a triangle cross-section and **Fig. 14** shows the variation of the longitudinal section (the section along the axial direction) of the workpiece during spinning [31]. When the forming height h ≤ 1.5 mm, the flange area of the blank remains upright without wrinkling, as shown in **Fig. 14**. However when 1.5 mm < h < 5.7 mm, the wrinkles occur at the flange area of the straight-side while the filleted-corner tilt backward. When 5.7 mm ≤ h ≤ 10.5 mm, more wrinkles appear at the flange area of the straight-side, while the filleted-corner becomes upright, as shown in **Fig. 15**. From h > 10.5 mm to the finish of spinning, the flange area at both of the straight-side and filleted-corner tilt forward, and the wrinkles are rolled over by the roller gradually when the roller moves over the blank. As reported by Cheng. et al. [32], during non-circular hollow-part spinning, the material flows from both sides of the filleted-corner to the straight-side, compressive stresses occur along the circumferential direction, as shown in **Fig.15,** which causing wrinkles to occur easily at the flange area of the straight-side.

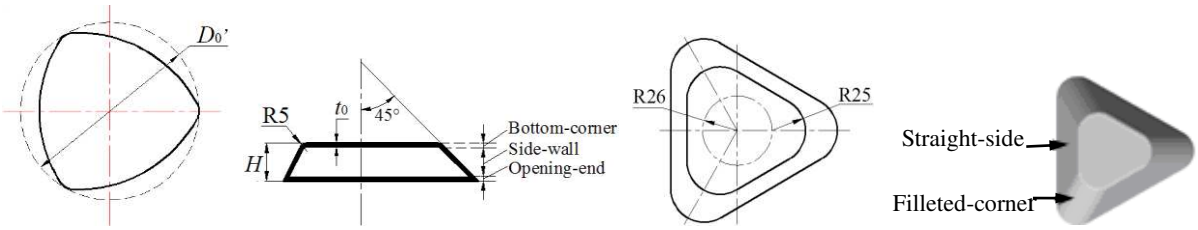

(a) blank. (b) axial section. (c) top view. (d) 3D model.

Fig. 13. Hollow part of triangular cross-section [33].

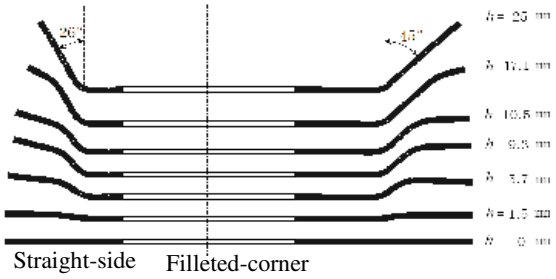

Fig.14 Deformation sequence of longitudinal cross-section of the workpiece during spinning [32].

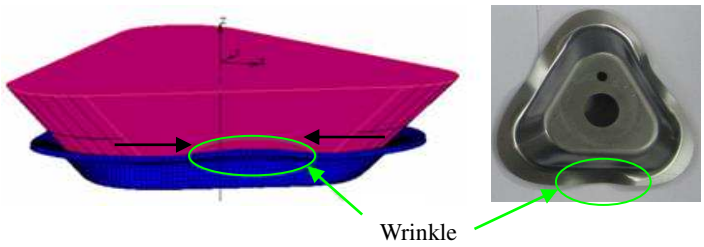

Fig.15. Wrinkle at straight-side [32].

As reported by Cheng, et al. [32], during non-circular hollow-part spinning with triangle cross-section, both equivalents stresses and strains periodically vary every 120º along the circumferential direction. There are obvious differences in magnitude of the equivalent stresses and strains between the straight-side and filleted-corner (**Fig.13(c)**). The maximum equivalent stress occurs at the opening-end, area A and B, as shown in **Fig. 16(a)**. The maximum equivalent strain occurs at the bottom-corner of the straight-side, area C, and the side-wall centre of the filleted-corner, area D, as shown in **Fig. 16(b)**.

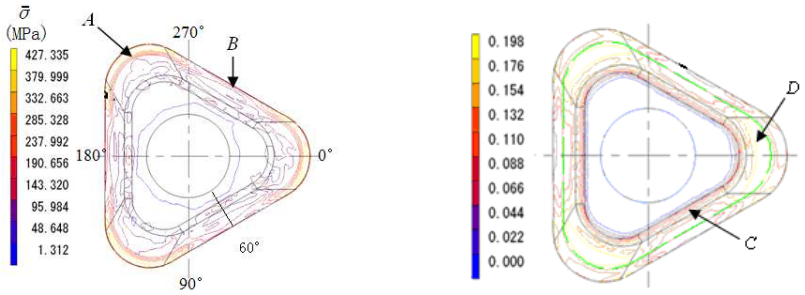

(a) equivalent stress. (b) equivalent strain.

Fig. 16. Distributions of equivalent stresses and strains [32].

To understand the variation of spinning forces during non-circular spinning, a hollow-part with triangular cross-section, as shown in **Fig. 13**, is selected as a case study and a series of experiments is carried out to measure spinning forces. The variation of spinning forces and the effect of the main processing parameters on the spinning forces are obtained using experimental measurement. An octagon ring transducer containing four octagon rings, as shown in **Fig. 17**, is designed and installed in the roller seat to measure the spinning forces. Three components of the spinning force along the radial, tangential, and axial direction of the roller can be measured by the octagon ring transducer. The roller is installed in the roller seat, 20 pieces of strain gauages are attached onto the surface of the octagon ring transducer. By this method, the spinning force components are measured and processed by computer and data acquisition software, as shown in **Fig. 18 [**33].

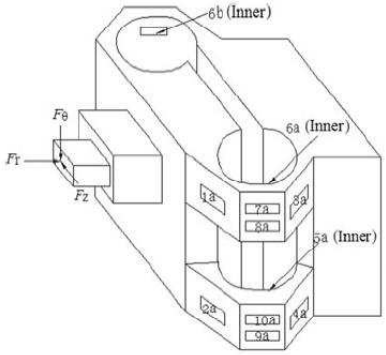

Fig.17. Octagon ring transducer [33].

1-Spinning mandrel 2-Spinning roller 3-Octagon ring transducer 4-Bridge wire 5-PC

6-Bridge box 7-Dynamic strain gauge 8-Numerical control system

Fig. 18. System used for measuring spinning forces [33].

In the spinning force measurement experiment, a one-path deep-drawing spinning process using a flat sheet blank is adopted, as shown in **Fig. 19**, where D_r, r_ρ and β' is the diameter, roundness radius and installation angle of the roller respectively, h is the height of forming part during spinning. The blank material is cold rolled steel sheet with thickness t_0=2 mm. As shown in **Fig. 20,** P_r, P_t and P_z is the three spinning force components measured by the octagon ring transducer along the radial, tangential and axial directions of the roller, when the roller feed rate f=0.4 mm/r, rotational speed of the mandrel n=60 r/min and thickness-diameter ratio of the blank t_0/D_0'=0.013, where D_0' is the diameter of the circumscribed circle of the blank, as shown in **Fig.13(a)** [33].

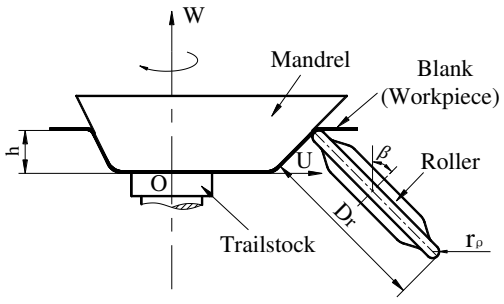

Fig. 19. One-path deep-drawing spinning [33].

Fig. 20 shows that similar to the conventional spinning (as reported by Wang et al. [34]) and the non-axisymmetric spinning (as reported by Xia et al. [35]), in the spinning of triangular cross-section hollow part the axial component of spinning force P_z is the greatest, the tangential spinning force P_t is the smallest and the radial spinning force P_r is the second highest. Different from the conventional spinning (as reported by Wang et al. [34]) but similar to the non-axisymmetric spinning (as reported by Xia et al. [35]), P_z, P_r and P_t vary periodically with the mandrel rotational angle. The experimental results also show that similar to the conventional spinning (as reported by Khamis Esa et al. [36]) and the non-axisymmetric spinning (as reported by Xia et al. [35]), the values of maximum spinning force (P_{zmax}, P_{rmax} and P_{tmax}) increase with the increase of the roller feed rate f. However different from the conventional spinning (as reported by Wang et al. [34]) and the non-axisymmetric spinning (as reported by Xia et al. [35]) processes, P_{zmax}, P_{rmax} and P_{tmax} increase with the increase of the mandrel rotational speed n in the spinning of triangular cross-section hollow part.

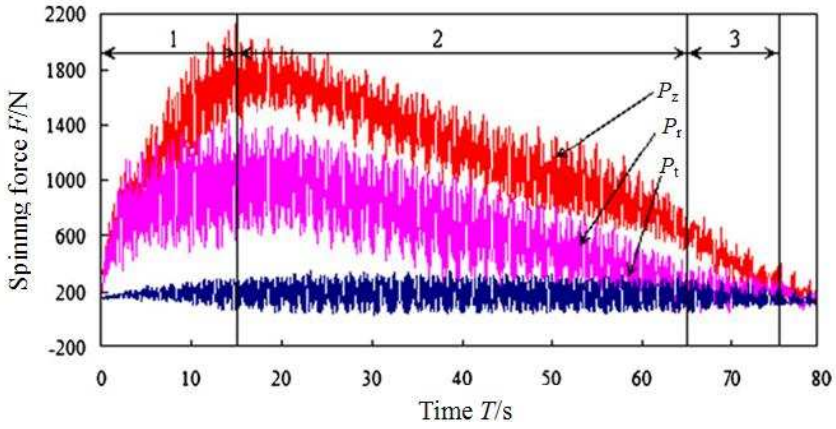

1-Bottom-corner 2-Side-wall 3-Opening-end

Fig. 20. Variation of spinning force components with time in spinning triangular cross-section hollow-part [33].

3.3. Tooth shaped spinning-Method 3

According to the variation of the wall-thickness of spun parts, the novel spinning processes can be divided into uniform wall-thickness spinning and tooth shaped spinning, the latter can be further subdivided into lateral tooth spinning and longitudinal tooth spinning, as shown in **Fig. 21**. In the lateral tooth spinning, the distribution of wall thickness is partially thickening and partially thinning along the axial direction after spinning, as shown in **Fig. 21(a)**.

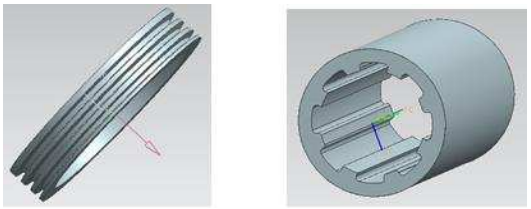

(a) lateral tooth spinning. (b) longitudinal tooth spinning.

Fig. 21. Lateral tooth and longitudinal tooth spinning.

3.3.1. Lateral tooth spinning

Belt pulley spinning is a typical example of application of the lateral tooth spinning process, as shown in **Fig. 21(a)**. As an important power transmission part, pulleys are widely used in automobile industry, agricultural machinery, pumps and machines. As reported by Packham et al. [37], pulleys are usually produced by machining after casting or forging, which lead to the disadvantages of material wastage, low production efficiency, low product dimensional accuracy resulting poor dynamic performance.

Recent development of spinning technology has enabled pulleys to be produced by spinning to replace casting and forging processes. **Fig. 22** shows one example of six-wedge poly-pulley used for automotive applications as reported by Cheng et al. [38]. As shown in **Fig. 22**, the wall-thickness of the tooth shaped portion of the pulley is at least 2.8+0.2 mm by split spinning, while the bottom thickness of pulley is only 2.5+0.2 mm. Therefore, a local thickening process has been developed to achieve near-net shape forming to reduce material wastage and number of manufacturing procedures required.

The whole manufacturing procedure of poly-wedge pulley spinning includes blanking, drawing and spinning processes, as reported by Cheng et al. [38]. The cup-shaped blank used for spinning is made by deep drawing process, as shown in **Fig. 23**. The spinning procedure includes five processes, performing, drumming, thickening, toothing and finishing, as shown in **Fig. 24**. The first process is performing by feeding the performing roller 1 along the radial direction together with the upper mandrel moving downward along the axial direction. The side wall of the cup-shaped blank obtained by deep drawning is deformed into the shallow drum-shaped workpiece, as shown in **Fig. 24(a)**. The second process is drumming by moving the upper mandrel downward individually until the bottom of the preformed shallow drum-shaped blank contacts with the lower mandrel tightly. The side wall of the shallow drum-shaped blank obtained by performing is further deformed into the deep drum-shape blank, as shown in **Fig. 24(b)**. The third process is thickening by feeding the thickening roller 2 along the radial direction until the side wall of the deep drum-shaped blank is flatened, as shown in **Fig. 24(c)**. The fourth process is tooth performing by feeding the toothing roller 3 along the radial direction to form the rough tooth profile, as shown in

Fig. 24(d). The final process is finishing by feeding the finishing roller 4 along the radial direction to shape the tooth profile accurately, as shown in **Fig. 24(e)**.

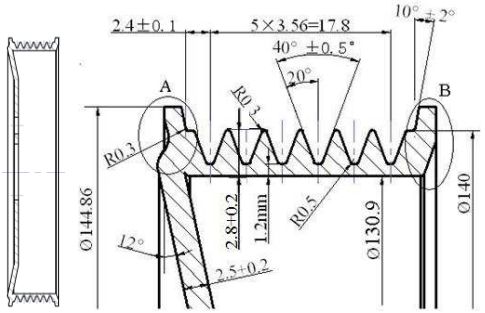

Fig. 22. Schematic of six-wedge poly-pulley [38].

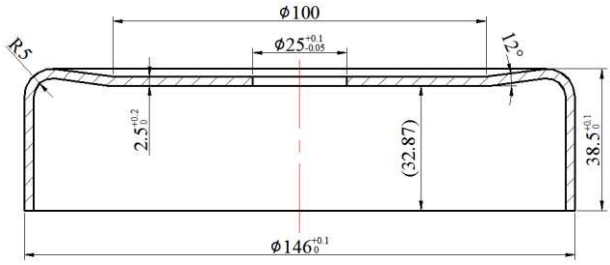

Fig. 23. Preforming drawing blank [38].

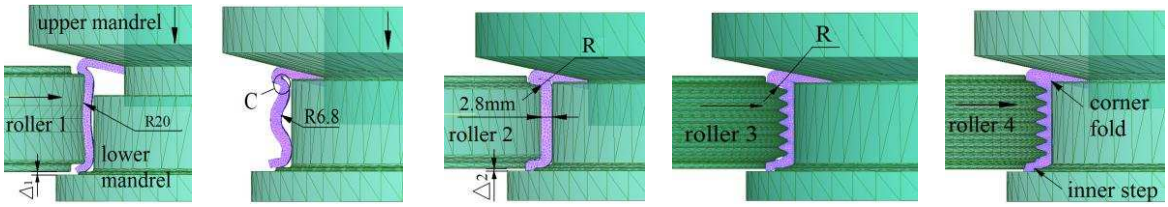

(a) preforming. (b) drumming (c) thickening (d) tooth preforming. (e) finishing.

Fig. 24. Schematic of five processes of poly-wedge pulley spinning [38].

As reported by Xia et al. [39], during performing, the maximum radial tensile strain occurs at necking area of performing blank, as shown in **Fig. 25(a)**. During drumming, bulging is the main deformation mode which occurs in the middle of drum-shape blank, therefore compressive strains occur in the inner layer of the bulging area and tensile strains occur in the outer layer, as shown in **Fig. 25(b)**. During thickening, tensile strains occur mainly in the radial direction while compressive strains occur mainly in the axial and tangential direction. As shown in **Fig. 25(c)**, the material flows into both ends of the blank along axial dircetion from the middle of the side-wall, behaves similarly as that in the radial compression and thickening.

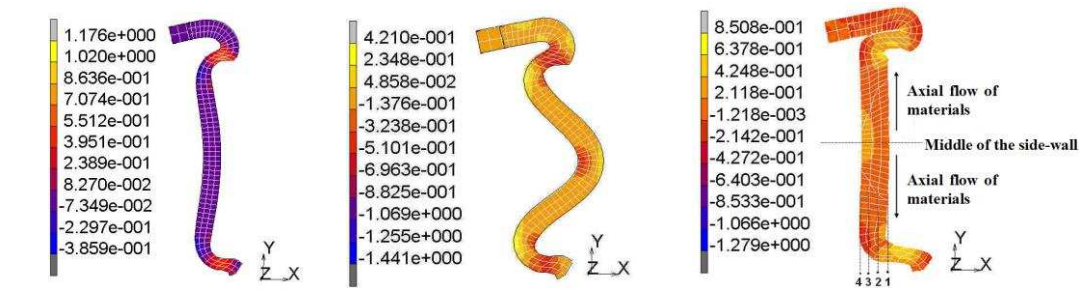

(a) preforming. (b) drumming (c) thickening

Fig. 25. Axial strain distributions during various processes of spinning [39].

3.3.2. Longitudinal tooth spinning

Longitudinal tooth spinning includes inner gear spinning and inner rib spinning [40]. The cup-shaped inner gears are widely used in the transmission with benefits of compact structure and light weight. They are usually produced by machining and welding, which results in multi stage manufacturing processes and long production cycle. As an incremental forming process, the inner gear spinning has the advantages of simple forming tools, low material wastage and reduced energy consumption, and low forming loads [41].

Xia et al. reported that during inner gear spinning [9], the material flowed along both the axial and radial directions, but also along the circumferential direction due to the partially thickening (in the area of gear-tooth) and partially thinning (in the area of tooth-groove), as shown in **Fig. 26**. **Fig. 27** shows the working principle of the thin-walled inner-gear stagger spinning using three rollers, where a certain distance is specified between rollers along both the axial and radial directions as reported by Xia et al. [42]. As shown in **Fig. 27**, the mandrel 2 with external shaped teeth is mounted on the spindle 1 of the machine; the cup-shaped blank 3 is placed on the mandrel 2 and fitted by the tailstock 4, which rotates together with the spindle and mandrel. The three rollers are uniformly distributed along the circumferential direction of the blank with 120° apart.

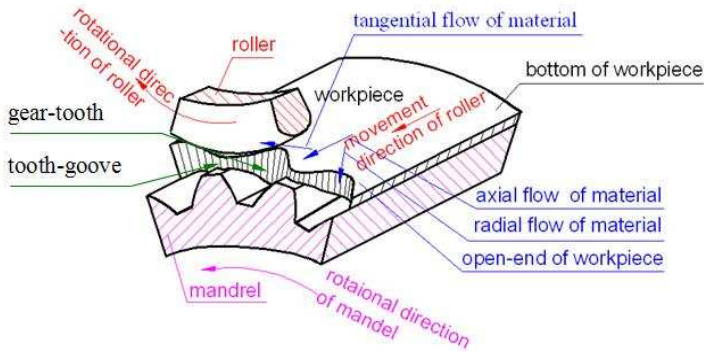

Fig. 26. Material flow of inner gear spinning [9].

In the cup-shaped inner gear spinning reported by Xia et al. [40], the rollers feed Δ along the radial direction

firstly, and then move from the bottom-end to the open-end of the blank along the axial direction. The teeth are formed on inner surface of the cup-shaped blank under the combined action of the roller and the mandrel.

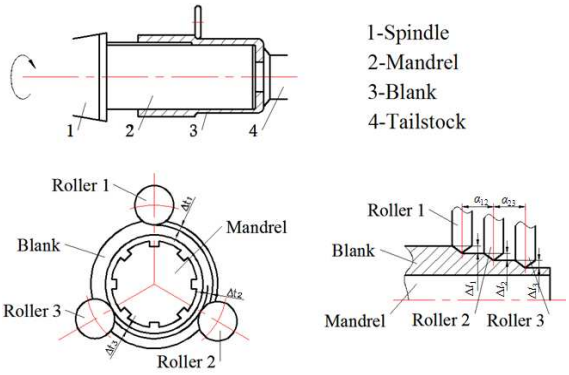

Fig. 27. Schematic of cup-shaped inner gear spinning [40].

As reported by Xia et al. [9], during the inner gear spinning, the material flows from the the bottom to the opening end of the cup-shaped workpiece along the axial direction. As shown in **Fig. 28(a)**, the axial flow of the material in the gear groove is greater than that in the gear tooth due to the radial constraint, which results in non-uniform material deformation between the gear tooth and gear groove. The radial flow of material is much more complex especillay in the inner-side of the workpiece, the material being extruded in the gear goove flows to the goove of the mandrel under the compression of roller resulting in the negative radial displacement, while the radial flow of material in the gear tooth is small, as shown in **Fig. 28(b)**. Along the circumferential direction, the volume of material flows from the outer surface to the inner surface is gradually decreased, as shown in **Fig. 28(c).** The material flow of the gear tooth, where the contact is firstly made with the roller, is the most important due to the fact that the circumferential constraint is the smallest.

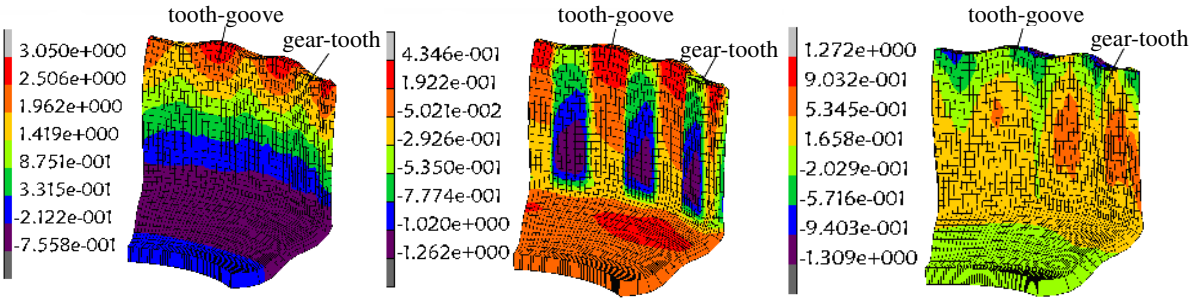

(a) axial direction (b) radial direction (c) circumferential direction

Fig. 28. Distributions of material displacement [9].

Summarizing the above three classification methods, the classification of the recently developed novel spinning processes is presented in **Fig. 29**.

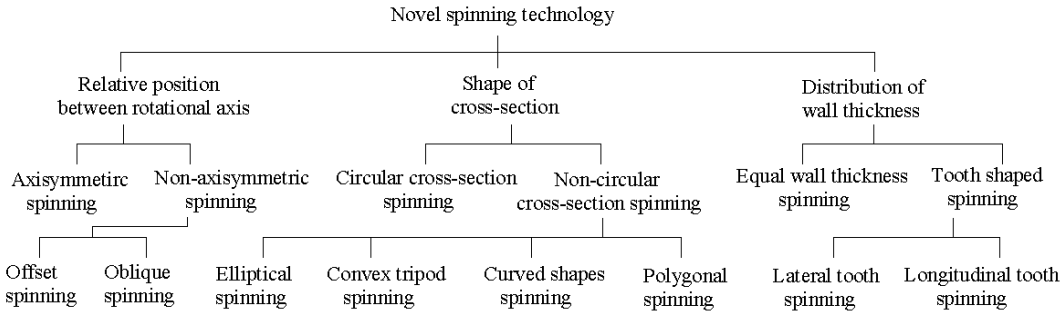

Fig. 29. Classification of novel spinning processes.

3.4. Discussion on other classification methods of novel spinning

In addition to the above proposed classification method of novel spinning processes, there are reports of other classification methods for novel spinning processes. Music et al. grouped the novel spinning processes as flexible spinning, asymmetric spinning and hot spinning [2]. In the authors' opinion, the classification of flexible spinning mentioned by Music et al. is similar to the conventional spinning or the shear spinning, which may be grouped by the following approaches, namely spinning a pre-formed shell [43], replacing the mandrel with a roller [16], spinning with a moving blank holder [44], spinning with a simple cylindrical mandrel [45] and spinning with a multi-roller tool set [2]. During the processes of spinning of a pre-formed shell [43], replacing the mandrel with a roller [16] and spinning with a simple cylindrical mandrel [45], the thicknesses of the workpiece obeys the sine-law, therefore these processes of mandrel-free spinning belong to shear spinning. In the other processes, the thickness of the workpiece undergoes minimal changes, thus these processes can be considered belonging to conventional spinning. The hot spinning is an old-age process and widely used technologe, especially in forming thick parts or hard-to-deform materials. During the hot spinning process, the nitrogen or inert gas is usually used as protective atmosphere which does not react with the workpiece, thus the mechanical properties of spun parts improve greatly due to the refining of the microstructure and the decreasing of the forming defects [18]. According to the deformation characteristics of material, the hot spinning can also be classified as conventional spinning and power spinning [18].

In recent years, some other novel spinning processes are also emerged. Sekiguchi et al. [46, 47] attempted to form conical parts with variable circumferential wall thickness through spinning; inclining the flange plane of the workpiece during the process was the fundamental strategy of this method. A part was formed as shown in sequence from (a) to (e) in **Fig. 30**, by maintaining the centripetal force F_Y parallel to the flange plane at a constant value using a force-control method and constraining the tip of the roller on the plane. Owing to the rotation of the workpiece on the spindle, the coordinate system used in the force/position control of the roller was

tilted depending on the inclination angle ϕ of the plane and the rotational angle of the spindle. By applying this method, it was predicted that the wall thickness distribution could be varied while retaining the same shape by altering the inclination angle of its flange plane during the process. The final wall thickness of a conical part was determined by the half-angle, inclination angle and the original thickness of the blank in accordance to the sine law [47]. Therefore this spinning method can be classified as shear spinning.

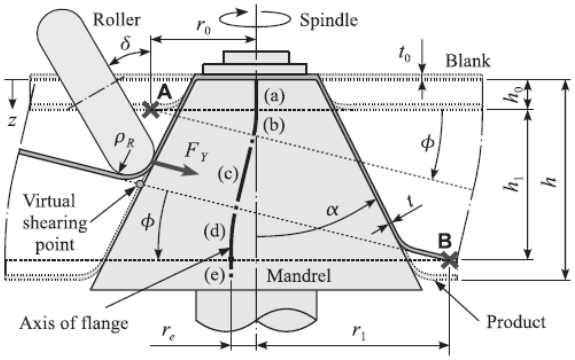

Fig. 30. Schematic of the experiment on controlling the wall thickness distribution in force-controlled shear spinning [47]. (α-half-angle; ϕ-inclination angle; t_0-initial thickness; t-final wall thickness; F_Y-centripetal force; z-axial position; h-height of product; h_0-initial forming height; h_1-oblique forming height; r_0-radial positionof point A; r_1-radial position of point B; r_e-estimated radial displacement of flange; ρ_R- roundness radius of tool; σ-tilt angle of roller).

4. Review of process advances and applications of novel spinning processes

Various novel spinning processes have been developed to produce a range of geometries in recent years. This section presents some examples of the development of novel spinning processes for industrial applications and analysis of tool design and their associated controls as well as spun part defects and material processing failures.

4.1. Non-axisymmetric spinning

Xia et al. [35] has successfully produced the offset parts (where various rotating axes are parallel to each other) and the oblique parts (there is a certain angle between the rotating axes) by using the non-axisymmetric spinning processes, without the need of post-processing such as welding. **Fig. 31** shows a typical automobile exhaust tube with offset axis on the left-end side and oblique axis on the right-end side, as reported by Xia et al. [20]. The traditional manufacturing method of the part is to separate the final geometry into three sections, the middle section of the circular tube (II) is welded with the two end tubes (I and III). Each of the end tubes are divided into two stamping parts from its center line (O_1-O_1 and O_2-O_2) respectively, then welded together. By using this traditional manufacturing method, not only the welding quality cannot be guaranteed but also the production cost is much higher because a number of the manufacturing procedures are required. By replacing the traditional

method with the spinning process, not only thermal distortions and potential fatigue cracks caused by welding can be avoided effectively; but also the mechanical properties and dimensional accuracy of tubes can be improved.

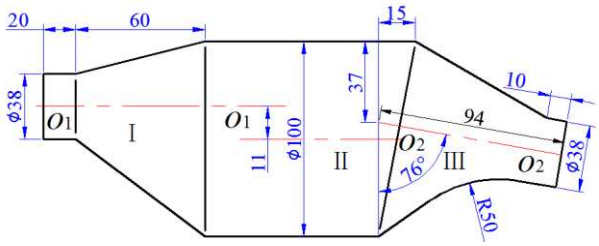

Fig. 31. Example of vehicle exhausts tube [20].

Xia et al. [35] developed the non-axisymmetric tube spinning process and associated equipment and tools, to manufacture non-axisymmetric thin-walled hollow parts with two or more rotational axes in one piece by using 6061 aluminium alloy tubes of 100 mm in diameter and 1.8 mm in thickness, as shown in **Fig. 32,** the deviation of wall thickness, straightness and ovality of spun part are 0.2 mm, 1.4 mm and 1.0 mm respectively. Comparing with the traditional manufacturing method, i.e., welding following stamping, the utilization of material increases from 70% to 90%, the production procedures are reduced from 10-passes to 2-passes. Therefore, the production cost is reduced significantly by spinning. Xia et al. [24] also developed a multi-function CNC spinning machine for the non-axisymmetric process, as shown in **Fig. 33**.

a) offset tubes. (b) oblique tubes. (c) tube with offset and oblique end

Fig. 32. Non-axisymmetric spun parts [35].

Fig. 33. HGPX-WSM multi-function CNC spinning machine [24].

As reported by Xia et al. [19], during the non-axisymmetric spinning, axial cracks may occur during multi-pass

neck-spinning due to the reduced ductility caused by material work-harding. **Fig. 34** shows an axial crack occurred during the 8th forward pass spinning when the nominal reduction of the blank radius per pass Δ_i is 4 mm. It shows that the fracture occurs at the initial spinning area during forward path spinning. **Fig. 35**(a) shows the spun workpieces produced by using different feed rates. **Fig. 35**(b) shows that all cracks locate at 0° area where the maximum deformation occurs. Because of the effect of work-hardening during multi-pass neck-spinning process, cracks occur if a small feed rate is adopted but can be avoided if appropriate spinning process parameters are selected.

Fig. 34. Occurance of crack if nominal reduction of blank radius Δ_i is too large [19].

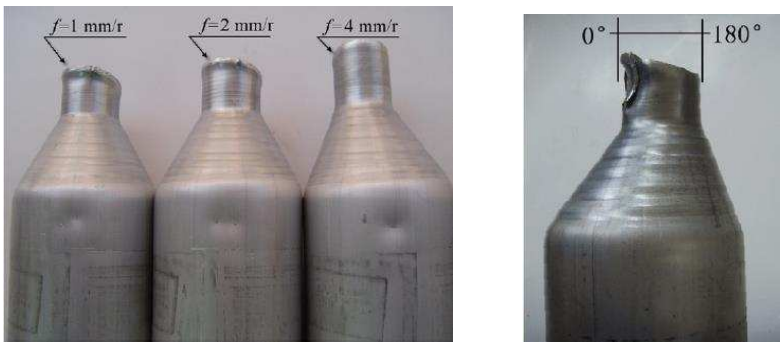

(a) spun workpieces using different feed rates f. (b) location of crack.

Fig. 35. Cracks at the opening end of the spun workpiece [19].

4.2. Non-circular cross-section spinning

Amano and Tamura reported a non-circular spinning method by using a radially offset roller on a modified spinning lathe to produce the hollow parts with elliptical cross-section [26]. Gao et al. developed another mechanical setup in which the spindle axis coincident with the revolution was offset [48]. In the experiment, the aluminium sheet of 1 mm in thicknesses is used as the blank. **Fig. 36** shows the spinning device and the spun workpieces of elliptical cross-section with Φ110 mm in long axis and Φ90 mm in short axis. As can be seen in **Fig. 36(a)**, the transmission shaft is installed on the holding chuck of a lathe at one end, while the holster is fixed onto

the slideway of the lathe. Two slide blocks are fixed onto the revolving drum. The three-jaw chuck is installed on the rotor disc, on which two orthogonal sliding chutes are attached. The slide blocks and the block mounted at the end of the shaft extend into the two sliding chutes and can slide along them. Therefore, the rotor disc and the revolving drum can be rotated by the lathe through the transmission shaft. The sheet blank is fixed onto the end surface of the mandrel by a supporting tail. The roller is installed in a small tool carrier of the lathe, so that the path of the roller can be controlled by the motion of the tool carrier. By changing the path of the roller, the spinning of parts with different elliptical shapes can be realized, and the maximum wall-thickness thinning ratio of spun workpiece is 16% [48].

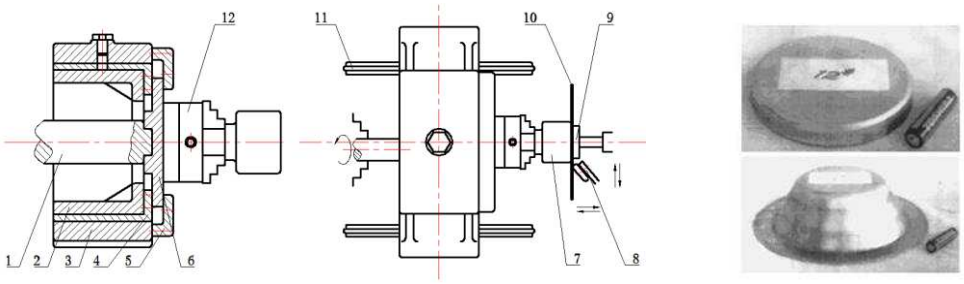

a) diagram of spinning machine. (b) elliptical spun parts.

1-transmission shaft 2-revolving drum 3-holster 4-slide block 5-clamping 6-rotor disc 7-elliptical mandrel 8-roller 9-supporting tail 10-blank 11-slideway 12-three-jaw chuck

Fig. 36. Elliptical spinning device based on two slide blocks and elliptical spun parts [48].

Arai [49] developed a novel metal spinning method based on hybrid position/force control for manufacturing non-circular cross-section parts and developed the corresponding equipment. The parts with quadrilateral roundness-type cross-section were successfully produced by using the pure aluminium (1050-O, annealed) sheet of 120 mm in diameter and 0.78 mm in thickness, as shown in **Fig. 37** [49]. Using this method, the roller is controlled by following the contour of the mandrel to force the material to deform onto the mandrel. This enables a non-axisymmentric spun part to be produced which bearing the same geometry as the mandrel, and the springback is small and the product tightly conforming onto the mandrel.

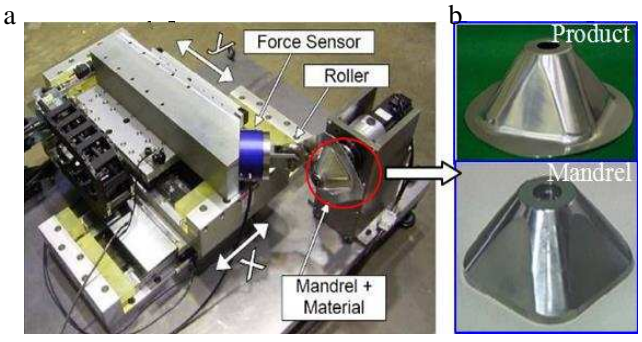

a) spinning machine. (b) spun parts.

Fig. 37. Linear motor driven metal spinning machine and spun parts [49].

Awiszus et al. developed a spinning method with a pair of diametrically opposite, spring-controlled rollers on a standard spinning lathe, and the parts with tripod shaped cross-section were successfully produced by using pure aluminium sheet of 120 mm in diameter and 1.5 mm in thickness, as shown in **Fig. 38 [6]**. The important factors which affect the distribution of wall-thickness of formed parts were investigated, and the non-circular cross-section parts with 24% wall-thickness thinning ratio were obtained by adopting the motion control of the rollers, and combining with the optimized forming processing parameters.

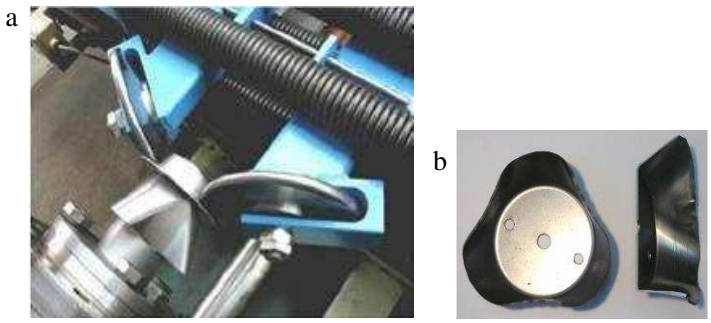

a) spinning device. (b) spun parts.

Fig. 38. Tripod shaped spinning device and spun parts [6].

Shimizu et al. developed a synchronous spinning machine, in which the rotational motion and feeding of the mandrel as well as the feeding of the rollers were controlled by the electric pulses to maintain the synchronization among the movements, as shown in **Fig. 39** [50]. The trajectory of the rollers was tracking controlled by software, which taking into account the effect of the deviation generated by step-by-step pulse control on spinning process; the elliptical cross-section parts were produced by using pure aluminium sheets of 1 mm in thickness.

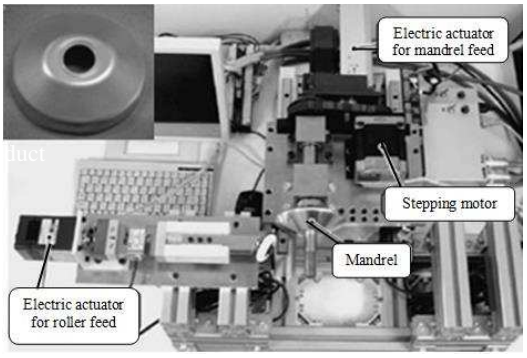

Fig. 39. Synchronous spinning device and elliptical cross-section spun part [50].

Sekiguchi et al. developed a spinning method which can be used to produce curved shapes and non-axisymmetric sectional shapes without using a dedicated die. A numerically controlled spinning lathe was

used to force the spherical head tool onto the prehemmed blank disc fixed on the spindle axis via a general purpose mandrel, with the tool moving along a trajectory which was calculated based on the desired shape. The fundamental strategy of the method was to move the tool along the axial and radial directions synchronously with the rotation of the spindle axis, to form the product according to the virtual curved axis instead of the real spindle-axis, as shown in **Fig. 40**. Since the flange plane of the workpiece is inclined from the normal plane of the spindle axis, the position of the roller and the angle of the spindle should be controlled synchronously. Various curved and non-axisymmetric sectional shapes of spun workpiece were obtained by using the pure aluminum sheets of 150 mm in diameter and 1.5 mm in thicknesses, and the maximum wall-thickness thinning ratio is 60%, as shown in **Fig. 41** [51].

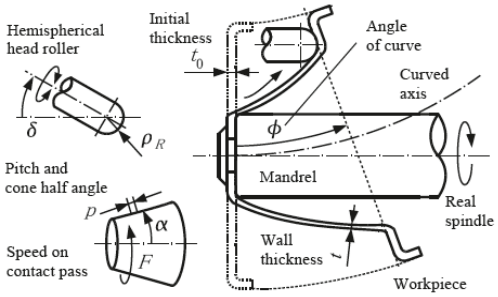

Fig. 40. Schematic of synchronous spinning of curved parts [51].

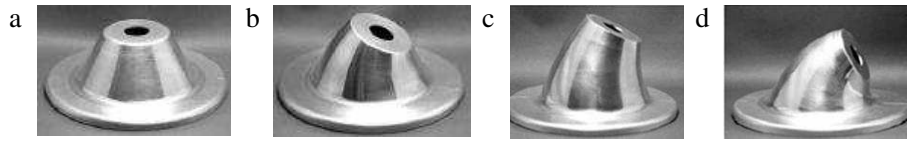

a) bending angle 0°. (b) bending angle 20°. (c) bending angle 25°. (d) bending angle 60°.

Fig. 41. Curved conical spun parts [51].

Xia et al. developed a spinning process based on profiling driving method to manufacture the polygonal non-circular cross-section parts and developed the corresponding spinning device, as shown in **Fig. 42 [33,52]**. The device consists of spinning mandrel 1, tailstock 2, worktable 3 (A), spinning roller 4, worktable 5 (B), profiling roller 6, profiling mandrel 7, guide strip 8, and gears 9. The spinning roller and the profiling roller are fixed on worktable B. The feed movement of the spinning roller is a resultant movement of the worktable A along Z-axis direction driven by a servo-actuator and the worktable B along a guide strip along X-axis direction driven by the profiling mandrel. The spinning mandrel and the profiling mandrel are driven by a pair of gears, rotated synchronously. The clearance between the spinning roller and the spinning mandrel is exactly controlled to the wall-thickness by the profiling mandrel. The complex tracking of the roller in 3D space is obtained by using

software ADAMS [52]. By using this method, several types of polygonal parts are produced, as shown in **Fig. 43**, such as (a) three straight-edges roundness-type produced by Lai et al. [30]; (b) triangle arc-type produced by Xia et al. [27]; (c) quadrilateral arc-type produced by Xia et al. [28]; (d) five straight-edges roundness-type produced by Xia et al. [29]. These non-circular parts with various cross-section are obtained by using the cold rolled steel sheet SPCC of 2 mm in thickness, the maximum wall-thickness thinning ratio is ranging form 14 to 24% and the springback angle is less than 2.2° [31, 53].

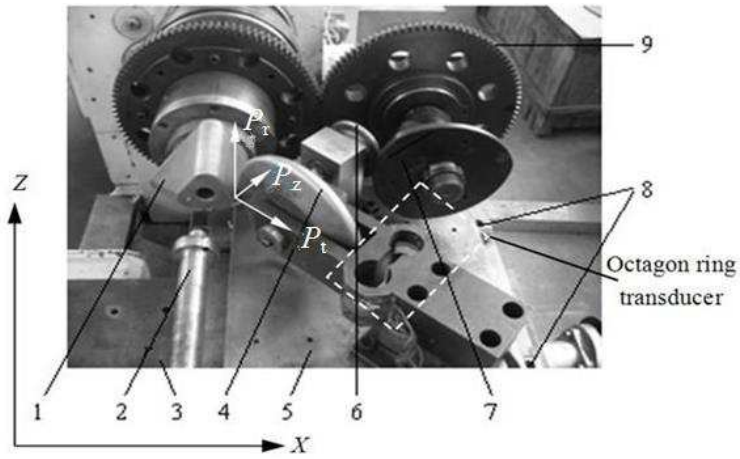

1-Spinning mandrel 2-Tailstock 3-Worktable A 4-Spinning roller 5-Worktable B 6-Profiling roller 7-Profiling mandrel 8-Guide strip 9-Gears

Fig. 42. Spinning device based on profiling driving method [52].

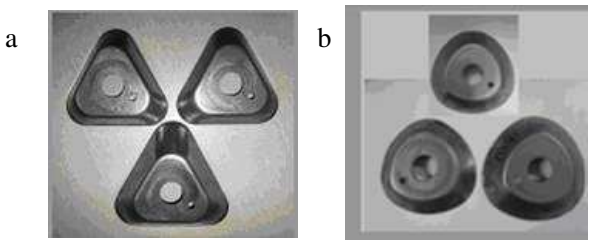

(a) three straight-edges roundness-type. (b) triangle arc-type.

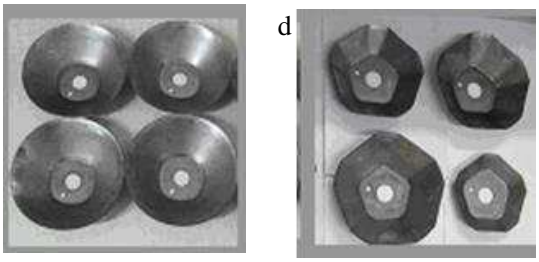

(c) quadrilateral arc-type. (d) five straight-edges roundness-type.

Fig. 43. Spun parts with non-circular cross-section [30,27,28,29].

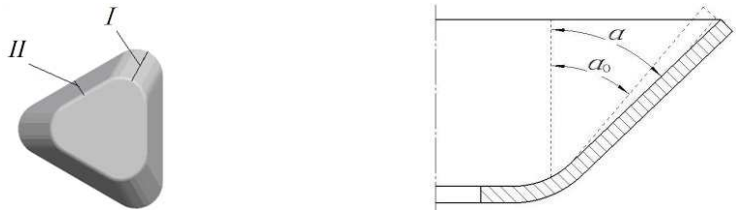

(a) intermediate generatrix. (b) springback angle.

Fig. 44. Evalution of geometrical accuracy [53].

Thickness uniformity and springback are two important indicators to evaluate the geometrical accuracy of spun parts of the non-circular cross-section spinning. Processing parameters affecting the spun part accuracy include: diameter of the roller D_r, roundness radius of the roller r_ρ, relative clearance between the mandrel and the roller ΔC ($\Delta C = 100\%(C-t_0)/t_0$, C is the clearance between the mandrel and the roller), rotational speed of the mandrel n and feed rate of the roller along axial direction f_z. As shown in **Fig. 44**, defining δ_t as the maximum wall thickness thinning ratio along the intermediate generatrix direction of the filleted-corner *I* or straight-side II surfaces; $\delta_t = 100\% \times (t_f - t_0)/t_0$, where t_f is the actual wall thickness of the workpiece. $\Delta\alpha$ is the springback angle of the workpiece, $\Delta\alpha = \alpha - \alpha_0$, where α is the semi-cone angle of the workpiece and α_0 is the semi-cone angle of the mandrel [53].

As reported by Xia [53], during non-circular hollow-part spinning with triangle cross-section, the effects of the relative clearance ΔC and the feed ratio of roller f_z on the maximum wall thickness thinning ratio δ_t are obvious, and the effects of the rotational speed of mandrel n and the diameter of roller D_r are slight; the effect sequence on the maximum wall thickness thinning ratio δ_t is the relative clearance ΔC, the feed ratio of roller f_z, the roundness radius of roller r_ρ, the rotational speed of mandrel n and the diameter of roller D_r. The effects of the roundness radius of roller r_ρ on the springback angle $\Delta\alpha$ is the most obvious, and the effects of the relative clearance ΔC and the diameter of roller D_r are slight; the influence sequence on the springback angle $\Delta\alpha$ is the roundness radius of roller r_ρ, the rotational speed of mandrel n, the feed ratio of roller f_z, the diameter of roller D_r and the relative clearance ΔC.

4.3. Tooth shaped spinning

4.3.1. Lateral-tooth spinning

For the manufacture of V-shaped pulleys, dynamic dampers and automobile wheels, blanks having cup shape on both sides are required [54]. An alternative forming method for such geometrical shapes is a special process of spinning, the so-called splitting process, as shown in **Fig. 45** [55]. This is performed by feeding a tapered roller

radially into a rotating disk blank. Initial research findings such as the conventional splitting process are documented in [56,57]. When manufacturing components by the conventional splitting process, several problems have been observed. Firstly, the process produces tensile stresses at the bottom of the split which can cause the formation of a crack. The severing material deformation frequently results in a crack preceding the splitting roller below the workpiece surface which then can cause production-related failure of the component in subsequent operation. Secondly, positioning the splitting roller and the disk blank relative to each other is problematic thus splitting of the workpiece will not take place necessarily parallel to the disk plane. The consequence of this is that different material thickness prevails in the angular areas. These process-bound disadvantages of the conventional splitting are to be eliminated by means of an innovative flow-splitting method developed by Schmoeckel and Hauk, as shown in **Fig. 46** [8]. By using this method, the tool configuration consists of three rollers, one splitting roller and two supporting rollers. While the splitting roller causes the material of the blank to flow into the two flange areas, the supporting rollers interact with the deformation zone of the blank underneath the deformation zone. The flange with a given wall-thickness can be formed by adjusting the distance between the splitting roller and each supporting roller. During the beginning of the forming process, the supporting rollers keep the blank from buckling. Once the edge of the blank undergoes deformation, the supporting rolls induce compressive stresses and thus increase the formability of the material.

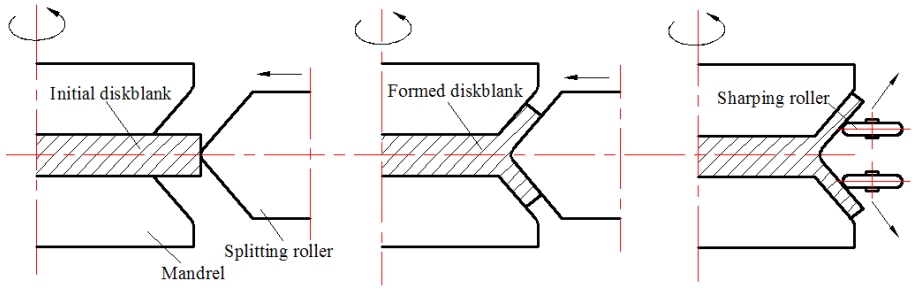

Fig. 45. Schematic illustration of splitting spinning process [55].

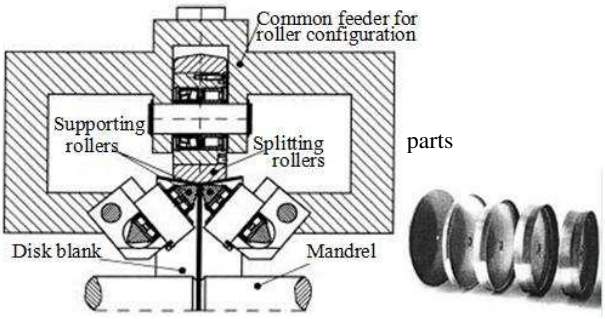

Fig. 46. Split spinning forming device and parts [8].

Cheng et al. developed a near-net shape forming process for manufacturing six-wedge belt pulleys by using 08AL steel sheets of 2.5 mm in thickness, as shown in **Fig. 47(a)** [38]. The required tooth shape and size can be formed directly by spinning without machining. Only minor machining procedure is required at the outlines as marked by A and B, as shown in **Fig. 22**. The deviation of the bottom diameter and the V-groove angle is 0.36 mm and 0.25°, respectively [38]. Comparing with the belt pulleys manufactured by machining after casting and forging processes, the material utilization by using spinning process increases from 40% to 70%. Furthermore, the spun pulley has inherent advantages, such as low manufacturing cost, improved material strength, thus prelonged service life. A vertical pulley spinning machine, HGQX-LS45-CNC is developed by Cheng et al., as shown in **Fig. 47(b)** [38]. The machine has an embedded system based on ARM (Advanced RISC Machines) which is used as the main CNC controller. The four mounting seats with different shapes of the rollers are driven by servo-motors.

However some defects may occur during the pulley spinning, such as diameter expanding at bottom section, flanging at opening end of the workpiece and unsymmetrical drumming during drumming process, as shown in Fig. 48. Side wall folding, insufficient bottom size and flash at opening end during thickening may also occur, as shown in Fig. 49 [38].

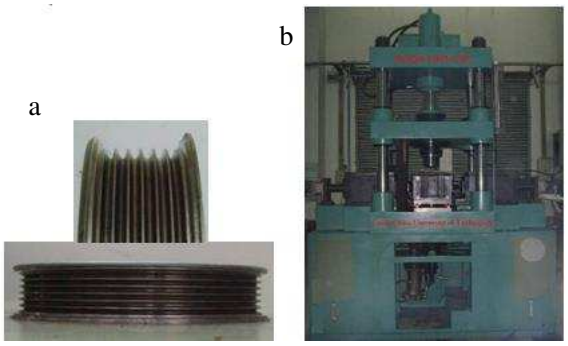

a) spun pulley. (b) HGQX-LS45-CNC spinning machine.

Fig. 47. Spun pulley and spinning machine [38].

The defect of diameter expanding at workpiece bottom section during drumming is shown in **Fig. 47(a)**, this is due to that the radial feed of roller 1 is too small, which should be at least 2 times of workpiece thickness; the defect of flanging at opening end during drumming is shown in **Fig. 48(b)**, this is due to that the setting height of roller 1 is inadequately selected; the defect of unsymmetrical drumming is shown in **Fig. 48(c)**, this is due to that the distribution of the side wall thickness of the cup-shaped workpiece obtained by deep drawing is uneven [38].

(a) diameter expanding (b) flanging (c) unsymmetrical drumming

Fig. 48. Defects during drumming process [38].

The defect of side wall folding is shown in **Fig. 49(a)**, a swallowtail along annular channel occurs on the side wall of workpiece during thickening. The reason for the defect is the existence of unsymmetrical drum during drumming process, as shown in **Fig. 48(c)**. The defects of insufficient bottom size and flash at opening end are shown in **Fig. 49(b)**. The reason for the defects is that the setting height of thickening roller is inapporitate [38].

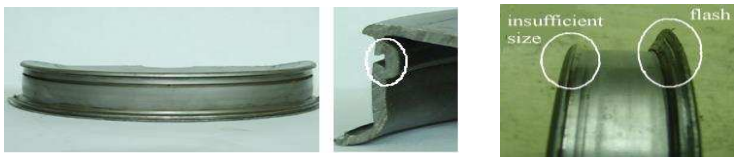

(a) side wall floding (b) insufficient size and flash

Fig. 49. Defects during thickening [38].

4.3.2. Longitudinal-tooth spinning

In recent years, considerable works have been carried out in longitudinal-tooth spinning. Xia et al. reported that the defects, such as the non-uniform distribution of tooth height along the axial and tangential directions and the wave-shaped opening-end of workpiece, are greatly affected by the processing parameters [42]. Sun et al. reported that the compressive deformation along tangential direction on the internal surface of part leads to a reduction in root circle of spun part, and the local loading and frictional effects result in the non-uniform radial deformation on the external surface of spun part [41]. Furthermore, in the work reported by Xia et al. [40], the process optimization is carried out by using the Response Surface Method (RSM) to obtain good dimensional accuracy of spun inner gears. A set of optimum processing parameters is obtained by taking the tooth fullness as the optimization target, and taking the thickness of circular blank and the reduction of wall-thickness of cup-shaped blank as the optimization parameters. Various spun inner gears are produced based on the selected optimum parameters by using the ASTM A36 steel steel tube of 76 mm in diameter and 2.5 mm in thickness, as shown in **Fig. 50** [58]. For the involute inner gear, the deviation of the tooth profile and spiral line, and the radial runout is 0.022 mm, 0.025 mm and 0.057 mm, respectively [40]. Spinning has shown a promising progress to become a new technique in gear manufacturing. It overcomes drawbacks of traditional machining processing, such as low

production efficiency, low precision and strict requirement for machining tools. By maintaining continuous material flow during deformation, the inner spun gear has improved fatigue strength, good wearability and prelonged service life. A stagger spinning device with three-rollers distributed uniformly along circumferential direction of the blank is developed by Xia et al., as shown in **Fig. 51** [58]. By using this device, the position of each roller can be adjusted individually both along the axial and radial directions.

a  b 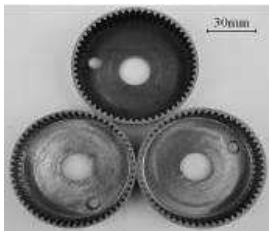

a) Rectangular inner gear. (b) Involute inner gear.

Fig. 50. Trapezoid and involutes inner gear spun parts [58].

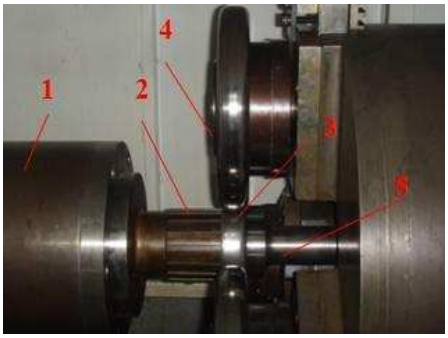

1- Spindle 2- Mandrel 3-Blank 4-Roller 5-Tailstock

Fig. 51. Stagger spinning device with three-rollers [58].

The spinning processes of tubular parts with longitudinal inner ribs are also extensively researched in recent years. The difference between these two types of spun parts is that there is no bottom on the end of the tubular parts comparing to the longitudinal inner ribs. Although the geometry of these two types of spun parts is similar, the application is very different. The use of inner gears is to transfer the motion and power, the forming quality of the inner gear is essential, especially the forming accuracy. However, the application of inner ribs is to enhance the stiffness and strength of tubular parts, only the accuracy of forming height of inner rib is required to be maintained.

Jiang et al. developed a backward ball spinning process to produce thin-walled tubular parts with longitudinal inner ribs. The tubular parts with six longitudinal inner ribs are produced, as shown in **Fig. 52** [59]. The height of ribs, the distributions, refinements and orientations of material grain sizes are simulated based on the rigid-plastic finite element methods, also by the design optimization of the ball dimension.

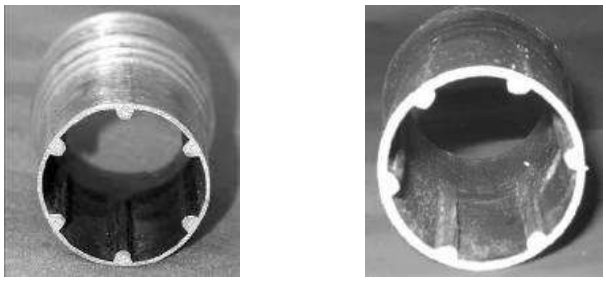

Fig. 52. Tubular spun product with inner ribs [59].

Some defects have been observered during the gear spinning, such as non-uniformly distribution of tooth height along axial and tangential direction, as shown in **Fig. 53** [42].

The tooth heigh is non-uniform distributed along axial direction when the radial reduction of wall-thickness is small, the spinning force is insufficient, or the formability of material plastic deformation is poor. For the non-deformed part of material close to the opening-end of the workpiece, its volume decreases with the proceeding of process, this results in a decrease of constraint force to the material flow along the axial direction. Consequently the material tends to flow along axial direction rather than along the radial direction; and tooth height gradually decreases from the bottom section to the opening-end of the workpiece, as shown in **Fig. 53(a)**. For a smaller radial reduction of wall-thickness, the material first contacts with the side of the space of tooth groove of the mandrel thus fill the area fully, and the space in the side to be contacted latterly is not filled fully (as shown in **Fig. 26**), which leads to a non-uniform distribution of the tooth height along the tangential direction, as shown in **Fig. 53(b)**. When the mandrel rotates, the contact area between the roller and the mandrel changes from gear-tooth of the mandrel to tooth-groove of the mandrel, which results in gradually decreasing of extrusion force applied to the material by the roller and the mandrel (as shown in **Fig. 26**). The volume of material flowing into the tooth-groove of the mandrel decreases correspondingly, which produces an uneven surface of the tooth tip.

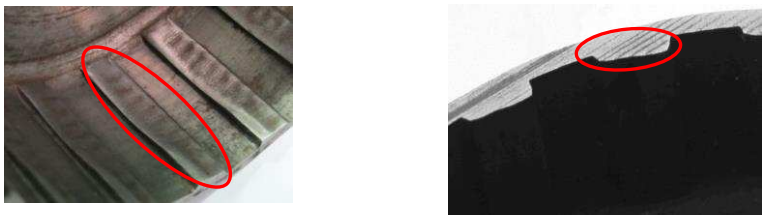

(a) axial direction (b) tangential direction

Fig. 53. Non-uniform distribution of tooth height [42].

5. Conclusions

In this paper, a classification method of metal spinning processes covering a broad range of spun part gemoetry

is presented, which not only includes the classification of traditional spinning processes, but also includes the novel spinning processes emerged in the recent years.

The traditional spinning processes are classified based on the deformation characteristics of material, the relative position between roller and blank, mandrel or mandrel-free spinning, and the temperature of the blank during spinning.

Recently developed novel spinning processes and equipment are reviewed in details, these include non-axisymmetric spinning, non-circular cross-section spinning, tooth shaped spinning. The classification of the novel spinning processes is proposed based on the relative position between rotational axes, the geometry of cross-section and the variation of wall-thickness of spun part. The development of these novel processes has allowed the spinning to be used for various new industrial applications.

The reviwed novel spinning processes are mainly used to manufacture the parts with complex geometries which have found applications in the automobile industry. The materials used in these novel spinning processes are mainly pure aluminium, aluminium alloy and low carbon steel tubes or sheets. Majoirty of the spun parts manufactured by the novel spinning processes have met the quality requirement of their specific applications. However, for high precision applications, the dimensional accuracy, such as the wall-thickness deviation of the non-circular cross-section parts, need to be further improved.

Recent researches of the novel spinning processes are mainly focus on the macro formability and the forming part quality, future prospects should be developing the controlling method of microstructure evolution during spinning and mechanical properties of the spun parts. Furthermore, in order to manufacture spun parts with high dimendional accuracy and good in-service performance, the integrated optimisation method of quality and performance of the spinning processes should be developed. Finally, the types of materials used in the novel spinning should be expanded, and the hot spinning process of the difficult-to-deform metal materials should be explored.

Acknowledgments

The research team would like to acknowledge the financial support of National Natural Science Foundation of China (No: 50275054, 50475097, 5077507, 51075153, 51375172); the Provincial Natural Science Foundation of Guangdong (No: 020923, 04105943, 10151040301000000); the Industrial Science and Technology Development Program Foundation of Guangdong (2003C102013, No: 600611901001); the Production, Teaching & Research Collaborative Project between Guangdong Province and Ministry of Education of China (Project No:

2006D90304021), GuangDong Province Key Laboratory of Precision Equipment and Manufacturing Technology (PEMT1202), and the EU Marie Curie Actions - MatProFuture Project (FP7-PEOPLE-2012-IRSES-318968).

References

[1] C.C. Wong, T.A. Dean, J. Lin, A review of spinning, shear forming and flow forming processes, International Journal of Machine Tools & Manufacture 43 (14) (2003) 1419-1435.

[2] O. Music, J.M. Allwood, K. Kawai, A review of the mechanics of metal spinning, Journal of Materials Processing Technology 210 (1) (2009) 3-23.

[3] E Hagan, J Jeswiet, A review of conventional and modern single-point sheet metal forming methods, Procedings of the Institution of Mechanical Engineers, Part B: Journal of Engineering Manufacture 217 (2003) 2 213-225.

[4] J. Jeswiet, F. Micari, G. Hirt, A. Bramley, Asymmetric single point incremental forming of sheet metal, CIRP Annals – Manufacturing Technology 54 (2) (2005) 623-649.

[5] Q.X. Xia, Investigation on the mechanism of the spinning technology of the 3D Non-axisymmetric parts, Chinese Journal of Mechanical Engineering 40 (2) (2004) 153-156. (In Chinese).

[6] B. Awiszus, F. Meyer, Metal spinning of non-circular hollow parts, in: Proceedings of the Eighth International Conference on Technology of Plasticity, October 2005, Verona, Italy, pp. 353-355.

[7] B. Awiszus, S. Hartel, Numerical simulation of non-circular spinning: a rotationally non-symmetric spinning process, Prod. Eng. Res. Devel. 5 (2011) 605-612.

[8] D. Schmoeckel, S. Hauk, Tooling and process control for splitting of disk blank, Journal of Materials Processing Technology 98 (1) (2000) 65-69.

[9] Q.X. Xia, M.H. Yang, Hu. Y, X.Q. Cheng, Numerical simulation and experimentation cup-shaped thin-walled inner rectangular gear formed by spinning, Chinese Journal of Mechanical Engineering 42 (12) (2006) 192-196. (In Chinese).

[10] K. Kawai, L.-N. Yang, H. Kudo, A flexible shear spinning of truncated conical shells with a general-purpose mandrel, Journal of Materials Processing Technology 113 (2001) 28-33.

[11] C.L. Packham, Metal spinning and shear and flow spinning, Sheet Metal Industries (1997) 382-398.

[12] M.S. Mohebbi, A. Akbarzadeh, A novel spin-bonding process for manufacturing multilayered clad tubes, Journal of Materials Processing Technology 210 (2010) 510-517.

[13] Wang Chenghe, Liu Kezhang, Spinning technology, Mechanical Industry Press, Beijing, 1986 (pp. 40-41).

(In Chinese).

[14] Kitazawa K, Wakabyashi A, Murata K, Yaejima K, Metal flow phenomena in computerized numerically controlled incremental stretch-expanding of aluminum sheets, Japan Institute of Light Metals 46 (2) (1996) 65-70.

[15] Chi-Chen Huang, Jung-Chung Hung, Finite element analysis on neck-spinning process of tube at elevated temperate, International Journal of Advanced Manufacturing Technology 56 (2011) 1029-1048.

[16] Shima S, Kotera H, Murakami H, Development of flexible spin-forming method, Journal of the Japan Society for Technology of Plasticity 38 (440) (1997) 814-818. (In Japanese).

[17] Y. Han, Z. Si, S. Wan, W. Wang, Q. Guo, J. Ma, Hot spinning technology for thickening the bottom from pipe billets, in: Proceedings of the Fourth International Conference of Rotary Forming, October 1989, pp. 109-113.

[18] Ken-ichiro, Minoru Ishiguro, Yuta Isomura, Hot shear spinning of cast aluminium alloy parts, Journal of Materials Processing Technology 209 (2009) 3621-3627.

[19] Q.X. Xia, S.W. Xie, Y.L. Huo, F. Ruan, Numerical simulation and experimental research on the multi-pass neck-spinning of non-axisymmetric offset tube, Journal of Materials Processing Technology 206 (1-3) (2008) 500-508.

[20] Q.X. Xia, X.Q. Cheng, H. Long, F. Ruan, Finite element analysis and experimental investigation on deformation mechanism of non-axisymmetric tube spinning, International Journal of Advanced Manufacturing Technology 59 (1-4) (2012) 263-272.

[21] Q.X. Xia, Y. Shang, S.B. Zhang, F. Ruan, Numerical simulation and experimental investigation on the multi-pass neck-spinning of non-axisymmetric oblique tube, Chinese Journal of Mechanical Engineering 44 (8) (2008) 78-84. (In Chinese).

[22] Q.X. Xia, S.J. Zhang, F. Ruan, Analysis on the spinning forces for 3D non-symmetrical thin-walled offset tubes, in: Proceedings of the Sixth International Conference on Frontiers of Design and Manufacturing, June 2004, Xi'an, China, pp. 111-113.

[23] Q.X. Xia, X.Q. Cheng, B.X. Liang, S.J. Zhang, F. Ruan, Analysis on the spinning forces for 3D non-axisymmetrical thin-walled oblique tubes, in: Proceedings of the Eighth International Conference on Technology of Plasticity, October 2005,Verona, Italy, pp. 577~578.

[24] Q.X. Xia, X.Q. Cheng, Y. Hu, F. Ruan, Finite element simulation and experimental investigation on the forming forces of 3D non-axisymmetrical tubes spinning, International Journal of Mechanical Science 48 (7) (2006) 726-735.

[25] Q.X. Xia, X.Q. Cheng, F. Ruan, Z.Y. Huang, Research on the forming forces during the 3D

non-axisymmetric thin-walled tubes neck-spinning, in: Proceedings of the International Technology and Innovation Conference, November 2006, Hangzhou, China, pp: 1686~1692.

[26] Amano T., Tamura K., Study of an elliptical cone spinning by the trial equipment, in: Proceedings of the Third International Conference on Rotary Metalworking Processes, September 1984, pp. 213–224.

[27] Q.X. Xia, Z.Y. Lai, X.X. Zhan, X.Q. Cheng, Research on spinning method of hollow part with triangle arc-type cross section based on profiling driving, Steel Research International (Special Edit) 81 (9) (2010) 994-997.

[28] Q.X. Xia, P. Zhang, X.Y. Wu, X.Q. Cheng, Research on distributions of stress and strain during spinning of quadrilateral arc-typed cross-section hollow part, in: Proceedings of 2011 International Conference on Mechanical, Industrial, and Manufacturing Engineering, January 2011, Melbourne, Australia, pp. 17-20.

[29] Q.X. Xia, Y.P. Wang, N. Yuan, X.Q. Cheng, Study on spinning of pentagonal cross-section hollow-part based on orthogonal experiment design, Advanced Materials Research 314-316 (2011) 783-788.

[30] Z.Y. Lai, Q.X. Xia, Z. Huang, X.Q. Cheng, Research on the roller feed track during spinning of hollow part with triangle cross-section, in: Proceedings of 2011 Second International Conference on Mechanic Automation and Control Engineering, July 2011, Inner Mongolia, China, pp. 649-652.

[31] X.Q. Cheng, X.Y. Wu, Q.X. Xia, Research on thickness distribution of spun hollow part with four arc-typed cross-section, in: Proceedings of the 10th International Conference on Technology of Plasticity, September 2011, Aachen, Germany, pp: 560-563.

[32] X.Q. Cheng, Z.Y. Lai, Q.X. Xia, Investigation on stress and strain distributions of hollow-part with triangular cross-section by spinning, International Journal of Materials and Product Technology 47 (1-4) (2013) 162-174.

[33] Q.X. Xia, Z.Y. Lai, Hui Long, X.Q. Cheng, A study of spinning force of hollow parts with triangular cross sections, International Journal of Advanced Manufacturing Technology 68 (2013) 2461-2470.

[34] Lin Wang, Hui Long, Investgation of material deformation in multi-pass conventional metal spinning, Materials and Design 32 (2011) 2891-2899.

[35] Q.X. Xia, B.X. Liang, S.J. Zhang, X.Q. Cheng, F. Ruan, Finite element simulation on the spin-forming of the 3D non-axisymmetric thin-walled tubes, Journal of Materials Science & Technology 22 (2) (2006) 261-268.

[36] Khamis Esa, Peter Hartley, Numerical simulation of single and dual pass conventional spinning processes, International Journal of Material Forming 2 (2009) 271-281.

[37] Packham C, Manufacture of one piece sheet metal V-belt pulleys with up to three grooves, Sheet Metal Industries 55 (4) (1978) 441-442.

[38] Cheng Xiu-quan, Wang Jia-zi, Xia Qin-xiang, Li Dong-he, Research on Forming Quality of Poly-wedge Pulley Spinning, in: Proceedings of the 11th International Conference on Manufacturing Research (ICMR2013), September, 2013, Cranfield, England, pp. 269-274.

[39] Q.X. Xia, J.Z. Wang, Y.P. Wang, Analysis on metal flow and deformation mechanism during thickening process of poly-wedge pulley spinning, Forging and stamping technology 34 (6) (2009) 101-106. (In Chinese).

[40] Q.X. Xia, L.Y. Sun, T. Xu, X.Q. Cheng, Parameter optimization of involute inner gear spinning based on response surface method, in: Proceedings of the 10th International Conference on Technology of Plasticity, September 2011, Aachen, Germany, pp. 564-567.

[41] L.Y. Sun, B.Y. Ye, Q.X. Xia, X.Q. Cheng, Analysis on forming characteristics of cup-shaped thin-walled inner gear spinning, Key Engineering Materials 455 (2011) 544-547.

[42] Q.X. Xia, L.Y. Sun, X.Q. Cheng, B.Y. Ye, Analysis of the forming defects of the trapezoidal inner-gear spinning, in: Proceedings of the International Conference on Industrial Engineering and Engineering Management, December 2009, Hong Kong, pp. 2333-2337.

[43] Kitazawa K., Wakabayashi A., Murata K., Seino J., A CNC incremental sheet metal forming method for producing the shell components having sharp components, Journal of JSTP 35 (406) (1994) 1348–1353. (In Japanese).

[44] S Matsubara, A computer numerically controlled dieless incremental forming of a sheet metal, in: Proceedings of the Institution of Mechanical Engineers Part B. Journal of Engineering Manufacture 215 (7) (2001) 959–966.

[45] K Kawai, L.-N Yang, H Kudo, A flexible shear spinning of truncated conical shells with a general-purpose mandrel, Journal of Materials Processing Technology 113 (1–3) (2001) 28–33.

[46] A. Sekiguchi, H. Arai, Development of oblique metal spinning with force control, in: Proceedings of 2010 International Symposium on Flexible Automation, July 2010, Tokyo, Japan, pp. 1863-1869.

[47] A. Sekiguchi, H. Arai, Control of wall thickness distribution by oblique shear spinning methods, Journal of Materials Processing Technology 212 (2012) 786-793.

[48] X.C. Gao, D.C. Kang, X.F. Meng, H.J. Wu, Experimental research on a new technology-ellipse spinning, Journal of Materials Processing Technology 94 (2) (1999) 197–200.

[49] H. Arai, Robotic metal spinning forming non-axisymmetric products using force control, in: Proceedings of the 2005 IEEE International Conference on Robotics and Automation, Barcelona, Spain, 2005, pp. 2691-2696.

[50] I. Shimizu, Asymmetric forming of aluminum sheets by synchronous spinning, Journal of Materials

Processing Technology 210 (4) (2010) 585-592.

[51] A. Sekiguchi, H. Arai, Synchronous die-less spinning of curved products, Steel Research International 81 (9) (2010) 1010-1013.

[52] Q.X. Xia, Y.P. Wang, Y. Ning, X.Q. Cheng, Parameters analysis of solving complex space tracks based on ADAMS, in: Proceedings of the The International Conference on Electrical and Control Engineering, June 2010, Wuhan, China, pp. 143-146.

[53] Q.X. Xia, Z.Y. Lai, J. X. Qu, X.Q. Cheng, Influence of processing parameters on forming quality of non-circular spinning, in: Proceedings of the 11th International Conference on Manufacturing Research (ICMR2013), September 2013, Cranfield, England, pp: 275-280.

[54] C. Packham, Manufacture of one piece sheet metal V-pullys with up to three grooves, Sheet Metal Industries 55 (1978) 441-445.

[55] Liang Huang, He Yang, Mei Zhan, 3D-FE modeling method of splitting spinning, Computational Materials Science 42 (2008) 643-652.

[56] D. Grotmann, Investigations on the rotationally kinematic forming of profile wheels, Dissertation, University Siegen, 1990. (In German).

[57] S. Keller, Static model for the determination of the force and torque required in the production of splitting discs, Hopner und Gottert, Siegen, 1996. (In German).

[58] X.Q. Cheng, L.Y. Sun, Q.X. Xia, Processing parameters optimization for stagger spinning of trapezoidal inner gear, Advanced Materials Research 189-193 (2011) 2754-2758.

[59] S.Y. Jiang, Y.F. Zheng, Z.Y. Ren, C.F. Li, Multi-pass spinning of thin-walled tubular part with longitudinal inner ribs, Transactions of Nonferrous Metals Society of China 19 (1) (2009) 215-221.